

## **Simulation Analysis and Experiment Study of Nanocutting with AFM Probe on the Surface of Sapphire Substrate by Using Three Dimensional Quasi-steady Molecular Statics Nanocutting Model**

**Zone-Ching Lin<sup>1</sup> and Ying-Chih Hsu<sup>1</sup>**

**Abstract:** The three-dimensional quasi-steady molecular statics nanocutting model is used by this paper to carry out simulation analysis of nanocutting of sapphire in order to explore the effects of conical tools with different tip radii of probe and straight-line cutting at different cutting depths, on cutting force. Meanwhile, this paper uses a cutting tool of atomic force microscopy (AFM) with a probe tip similar to a semisphere to conduct nanocutting experiment of sapphire substrate. Furthermore, from the experimental results of nanocutting sapphire substrate, this paper innovatively proposes the theoretical model and equation that the specific down force energy (SDFE) during nanocutting by using AFM probe as the nanocutting tool, is approximately a constant value. This paper uses three-dimensional quasi-steady molecular statics nanocutting model to simulate calculation and obtain nanocutting down force. It is compared with the down force calculated by SDFE theoretical equation proposed for verification. As a result, the down force obtained by the paper's simulation is very close to the down force calculated by SDFE theory. Therefore, it can be verify that the three-dimensional quasi-steady molecular statics nanocutting theoretical model used by this paper is feasible. The SDFE proposed by this paper is defined as equating to down force energy dividing the removed volume of down press of the workpiece by the AFM probe. From the experimental data and the calculation results, it is found that the values of SDFE under different down force actions are almost close to a constant value. The three-dimensional quasi-steady molecular statics nanocutting sapphire workpiece model is to find the trajectory of each atom of the sapphire workpieces being cut whenever the diamond cutter goes forward one step. It uses the optimization search method to solve the force equilibrium equation of the Morse force in the X, Y and Z directions when each atom moves a small distance, so as to find the new movement position of each atom, and step by step calculates the behavior during cutting.

---

<sup>1</sup> Department of Mechanical Engineering, National Taiwan University of Science and Technology, Taipei, Taiwan.

**Keywords:** quasi-steady molecular statics, specific down force energy (SDFE), atomic force microscopy(AFM), nanocutting.

## 1 Introduction

The theory of molecular mechanics was first proposed by Irving and Kirkwood (1950). It mainly entails the use of a potential energy function model that dominates the action force between molecules, and the calculation of movement equation to acquire the corresponding physical properties and dynamic characteristics. The theory of molecular mechanics is mainly composed of three parts: (1) potential energy selection model; (2) Newton movement equation, and (3) energy minimization method. Of them, the method used by scholars applying Newton movement equation is called molecular dynamics (MD), whereas the method used by scholars applying energy minimization for calculation is called molecular statics (MS). The purpose of both of them is to find the displacement of each molecule in the system according to the action force on the molecules in the system and the initial position status.

Shimada (1990) used 2D models and molecular dynamics to perform dynamic simulation of orthogonal cutting and explore its relationship with the formation of chips. Childs and Maekawa (1990), Belak and Stower (1990) employed MD theory for numerical simulation of cutting, but their model lacked complete quantitative calculation. Fang, Wu, Zhou and Hu (2007) indicated that the nanoscale cutting action was mainly produced by extrusion, unlike the traditional cutting behavior that shear force made workpiece become deformed. Inamura and Takezawa (1991, 1992) considered atoms as nodes, and used the Morse potential between atoms to deduce the finite element formulation of an atomic model. They took the Morse potential between two different atoms as examples for simulation, and acquired the formation process of chips, as well as the changing process of shear force and potential energy with the movement of cutting tool. Lin and Huang (2004) improved the finite element model of Inamura, Takezawa and Kumaki (1993), and used the Morse potential between cutting tool and workpiece atoms to govern atomic movement by MD so as to describe the entire cutting process. With atoms regarded as nodes and lattices as elements, they developed a nanoscale orthogonal cutting model equation, and calculated the displacement of each molecule on the middle cross-section of the cut workpiece. Using the calculated molecular displacement and the concept of shape function in FEM, they calculated the strain of material. Furthermore, they used the flow stress-strain relational equation obtained after regression of the stress-strain curve of numerical stretching experiment of nanoscale thin film, to calculate equivalent stress. Cai, Li and Rahman (2007) used the radius of the same cutting tool to explore different cutting depths of silicon workpiece,

and made simulation comparison among different cutting depths and tip radii of cutting tool. As a result, two important conclusions were drawn. When cutting of Si material was performed in ductility model, the cutting depth had to be smaller than the radius of cutting tool. When the cutting tool was greater than a certain limit, ductility cutting could not be produced. Therefore, the radius of cutting tool had to be appropriately small for smooth cutting.

Nevertheless, since the time step of MD was too small, a great deal of time had to be spent on calculation during the simulation process, thus creating problems surrounding difficult calculation. Therefore, there were scholars who gradually took molecular statics method to simulate nanoscale studies, with the expectation to improve the problems encountered in MD. Kwon and Jung (2004) explored the material nature of atomic scale balance in static load, and proposed a model combining atoms and FEM. This model was used to simulate the stretching problem of nanoscale on materials with defects. Using molecular statics (MS) method, Jeng and Tan (2004) took the smallest energy principle in finite element as the structure in order to simulate the displacement and deformation process of nanoscale impress. The smallest potential energy method was mainly used. After that, displacement control iterative method in non-linear FEM was used to solve the relationship between different forces and positions of atoms. Lin and Ye (2009) used 2D nanocutting molecular statics model to simulate cutting the copper material and analyzed the cutting action. However, this paper didn't consider the conditions of three dimension nanoscale cutting. Lin and Wang (2010) used 3D quasi-steady molecular statics to simulate and investigate the abrasive cutting behavior on silicon wafer, and compared the simulation results with the related literature of using molecular dynamics method to prove the 3D quasi-steady molecular statics nanoscale abrasive cutting model is reasonable.

In general, AFM was used for measurement and observation of surface morphology. With the properties of simple setting, fast operation and high resolution, AFM became feasible equipment for machining minute parts and microstructure. And applying AFM probe as a machining and cutting tool to carry out mechanical cutting had been proved by related scholars as a rather useful technique in the machining of nanoscale microstructure on semiconductor, photoelectric element and metallic surface [Tseng, Jou and Notargiacomo (2008)]. Fang, Weng and Chang (2000) used AFM probe to conduct nanoscale scratching experiment of silicon substrate coated with aluminum film. Experimental results showed that scratching depth deepened with the load of probe and scratching cycles, and the normal force of press of the probe tool had the most obvious effect. Wang, Jiao, Tung and Dong (2010) used AFM to machine nano channel on the surface of Si oxide, and performed experiment to explore how the normal force of press is related to cutting

speed and cutting depth. The experiment of scratching Si wafer by AFM probe tool conducted by Tseng (2010) also showed that the depth and width of scratching ditch increases with the increase of the down force and scratching cycles of probe. Through regression of the experimental data, it is known that the relationship between the dimensions of nano ditch machined by AFM probe and the normal force of probe's press is in logarithmic form, and the relationship between the former and scratching cycles is in power-law form.

Sapphire ( $\text{Al}_2\text{O}_3$ ) has a rhombohedral structure. Since its optical penetration band is very wide, it has very good transmittance. Therefore, sapphire has been extensively applied to optical elements. Besides, also because of its thermostability and high degree of hardness, it is also a difficult material for machining. Currently, there is still no related literature studying the use of sapphire to be a material for nano machining. Hence, this paper focuses its research on the use of AFM probes as they are used to carry out nanoscale cutting. Different from the traditional way of electrochemical etching, this paper conducts the experiments of machining V-shaped groove on the surface of sapphire substrate by using AFM and the studies its microstructure. For general related academic references about three-dimensional nanocutting, their simulation analyses mostly used MD model. However, this method needs analysis and simulation for a long time. As for molecular statics nanocutting model and the use of AFM to carry out cutting and machining of nano groove on sapphire substrate, currently there is still no literature to combine with molecular statics nanoscale cutting theory and related of experimental verification. Therefore, this paper establishes a simulation model of three-dimensional quasi-steady molecular statics nanocutting of sapphire. Focusing on different tip radii of probes of AFM's conical tool and different cutting depth, this paper conducts simulation and analysis of different axial cutting forces. From the actual nanocutting experimental data, and according to the specific down force energy theoretical equation developed by this paper, this paper analyzes the relationship between down force and cutting depth as well as the relationship between cutting passes and cutting depth. Finally, this paper uses three-dimensional quasi-steady molecular statics nanocutting model to simulate calculation and obtain nanoscale cutting down force. The calculated result is compared with the down force calculated by the specific down force energy (SDFE) theoretical equation proposed which is verified by the experimental result of actual nanocutting of sapphire substrate by AFM probe. After comparison, it is found that the down force acquired from the simulation result of this paper is close to the down force acquired from calculation by SDFE theory. Therefore, it can be verified that the three-dimensional quasi-steady molecular statics nanocutting theoretical model for cutting sapphire substrate used by this paper is feasible.

## 2 Three-dimensional quasi-steady molecular statics simulation of nanocutting

### 2.1 Nanocutting sapphire substrate simulation model

This paper uses three-dimensional quasi-steady molecular statics nanocutting model to simulate the cutting of a sapphire ( $\alpha\text{-Al}_2\text{O}_3$ ) workpiece using AFM diamond probe. The physical model of nanocutting is composed of 56,079 to 138,600 sapphire atoms arrayed in a hexagonal close-packed structure, and belongs to a rhombohedral structure, as shown in Fig. 1. The cutting tool is composed of 2,623 to 9,615 carbon atoms and arrayed in a diamond formation.. Thus, this paper carries out simulation use of the conical tool of AFM probe to establish a three-dimensional quasi-steady nanocutting model of molecular statics and perform cutting of sapphire substrate. The calculation parameters of cutting are shown in Table 1. The model of three-dimensional nanocutting of sapphire crystal structure is shown in Fig. 1. It is found that building the model of three dimensional sapphire crystal structure as Fig. 1 is more difficult than building the model of three dimensional monocrystalline silicon structure. The nanoscale cutting was simulated by displacing the diamond tool a small distance towards the negative direction of the X-axis, as shown in Fig. 2.

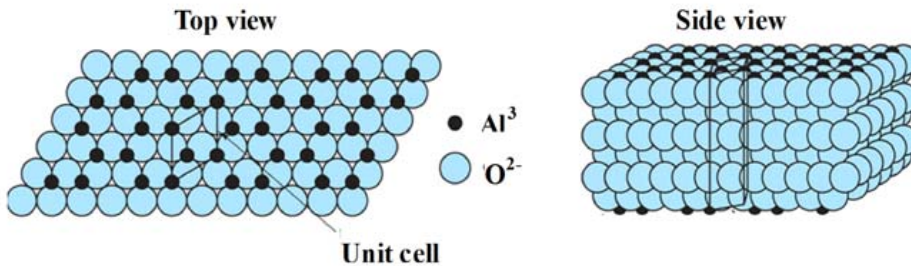


Figure 1: Crystal structure of  $\alpha\text{-Al}_2\text{O}_3$  (James F. Shackelford, 1988)

### 2.2 Three-dimensional quasi-steady molecular statics nanocutting simulation model

The three-dimensional quasi-steady molecular statics nanocutting model of this paper uses the adopts Morse potential energy of two-body potential energy as the basis for calculation of the action force between molecules. The equation of Morse

Table 1: Calculation parameters for simulation nanocutting of sapphire substrate by molecular statics

Configuration	Nanocutting	
Sapphire (workpiece material)	$30a \times 10a \times 15c$	$15a \times 8a \times 15c$
$a$ and $c$ are the lattice constant of sapphire		
( $a = 4.759 \text{ \AA}$ , $c = 12.991 \text{ \AA}$ )		
Number of atoms in Sapphire	138,600	56,079
Number of atoms of tool (rigid-body diamond)	9,615	2,623
Tip radius of tool (nm)	5	2
Depth of cut (nm)	0.5	0.4, 0.5, 0.6

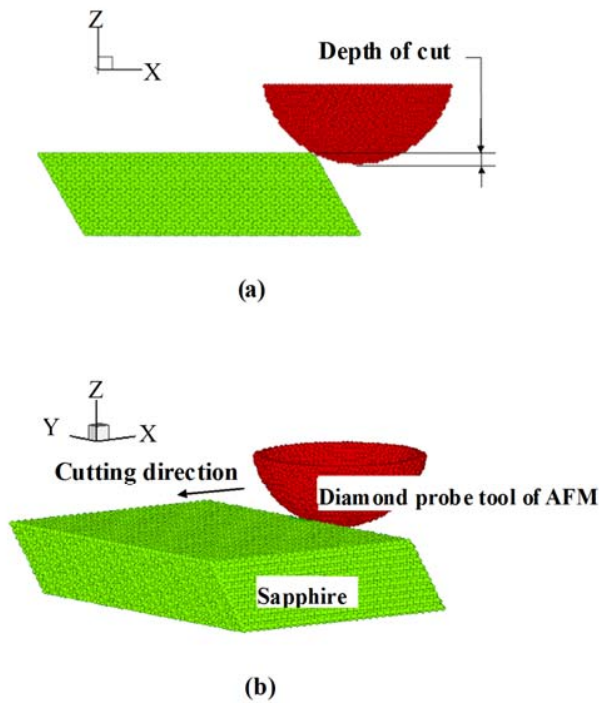


Figure 2: Simulation model for nanocutting of sapphire substrate: (a) side view, (b) 3D image.

potential energy [Girifalco and Weizer (1959)] is expressed as follows:

$$\Phi(r_{ij}) = D \left\{ e^{-2\alpha(r_{ij}-r_0)} - 2e^{-\alpha(r_{ij}-r_0)} \right\} \quad (1)$$

where  $\Phi(r_{ij})$  is a pair potential energy function,  $D$  is the cohesion energy,  $\alpha$  is the elastic modulus,  $r_{ij}$  is the distance between two atoms and  $r_0$  is the particle distance at equilibrium.

For the general potential energy function, when the distance between two atoms is greater than a certain distance, the action force between these atoms will decrease rapidly. Therefore, we define such distance cut-off radius  $r_c$ , and when the distance exceeds  $r_c$ , the action force is very small so it does not need to be calculated. In this way, the calculation can be tremendously simplified. Therefore, when the distance between two atoms is within  $r_c$  and beyond  $r_c$ , Morse potentials can be furthered expressed as equation (2):

$$\begin{cases} \Phi(r_{ij}) = D \left\{ e^{-2\alpha(r_{ij}-r_0)} - 2e^{-\alpha(r_{ij}-r_0)} \right\} & r \leq r_c \\ \Phi(r_{ij}) \cong 0 & r > r_c \end{cases} \quad (2)$$

This paper adopts Morse's two-body potential energy function to describe the interaction force between the molecules when the diamond cutter is cutting the sapphire workpiece. Since the atomic lattice structure of sapphire is more complicated than the single crystal structure of a single atom, and this paper takes an AFM diamond probe as a cutting tool to cut sapphire ( $\alpha$ - Al<sub>2</sub>O<sub>3</sub>), the relationship between C atoms of diamond probe and the atoms of sapphire ( $\alpha$ - Al<sub>2</sub>O<sub>3</sub>) workpiece has to be considered. From Table 2, the potential energy parameters, including Al-Al [Girifalco and Weizer (1959)], O-O [Graves and Brault (2008)] and C-C [Maekawa and Itoh, 1995], are all known. As to the Morse potential parameters among different atoms, such as Al-C, Al-O and O-C, the study uses Lorentz-Berthelot mixing rule (1986) to calculate Al-C, Al-O and O-C Morse potential parameters, which are taken as the parameters of the nanocutting model simulated by this paper. The calculated numerical results of the Morse potential energy parameters among different atoms are shown in Table 2. From Table 2, it can be found that the equilibrium distance of aluminum atoms is larger than that of oxygen atoms for the sapphire, thus this paper uses 2.5 times the equilibrium distance of aluminum atoms of the sapphire as the cut-off radius.

Table 2: Morse potential parameters for cutting of sapphire workpiece by AFM diamond probe tool

	Al-Al	O-O	C-C	Al-O	Al-C	O-C
D: (eV)	0.27	5.12	2.423	0.912	0.28	3.522
$\alpha$ :( $\text{\AA}^{-1}$ )	1.165	2.68	2.555	0.717	2.78	2.617
$r_0$ : ( $\text{\AA}$ )	3.253	1.208	2.522	2.231	2.20	1.865

According to the Morse potential used by this paper, the negative value of Morse potential gradient is taken to find the action force of molecules, which is expressed as equation (3):

$$F(r_{ij}) = -\frac{\partial\Phi(r_{ij})}{\partial(r_{ij})} = 2D\alpha \left\{ e^{-2\alpha(r_{ij}-r_0)} - e^{-\alpha(r_{ij}-r_0)} \right\} \quad (3)$$

As inferred from equation (3), the expression of action force between atoms is shown in equation (4):

$$\vec{F}_i = \sum_{j=1}^n \vec{F}_{ij}(r_{ij}) \quad (4)$$

where  $i$  is the code number of diamond probe's atom;  $j$  is the code number of oxygen atom and aluminum atom in workpiece;  $n$  is the number of workpiece atoms; and  $r_{ij}$  is the distance between two atoms.

After action force is obtained, cut-off radius method is used to additionally judge whether the distance of  $r_{ij}$  is greater than the parameter  $\delta$  of  $r_c$ . Equation (4) is rewritten as equation (5) in order to judge whether it is greater than  $r_c$ . When the distance of  $r_{ij}$  is greater than  $r_c$ , there is almost no potential energy action, so that let  $\delta$  be zero. Contrarily, when the distance of  $r_{ij}$  is smaller than  $r_c$ , action force will be produced. By then, let  $\delta$  be 1, and then calculate the action force between atoms.

$$\vec{F}_i = \sum_{j=1}^n \vec{F}_{ij} \delta(r_{ij}) \quad (5)$$

$$\begin{aligned} \text{if } r_{ij} > r_c &\Rightarrow \delta = 0 \\ \text{else } r_{ij} \leq r_c &\Rightarrow \delta = 1 \end{aligned}$$

The numerical value of the action force produced is divided into three axial component forces,  $F_x$ ,  $F_y$  and  $F_z$ , with their relationship expressed in equation (6).

$$\vec{F}_i = \vec{F}_{x_i} + \vec{F}_{y_i} + \vec{F}_{z_i} \quad (6)$$

where  $F_{x_i}$  is the component force of action force in X direction;  $F_{y_i}$  is the component force of action force in Y direction; and  $F_{z_i}$  is the component force of action force in Z direction.

When the action forces in three axial directions produced from  $n$  grains of atoms in material being applied on  $m$  grains of probe atoms on cutting tool are added up, the total component forces in three axial directions can be obtained.  $F_x$  is the cutting

force produced by diamond probe during cutting;  $F_z$  is the down force of diamond probe during cutting; and  $F_y$  is the side force of diamond probe and workpiece.

Of course, after cutting has proceeded for a certain period, the number of workpiece atoms affected by Morse force of diamond cutting tool is not only one atom. Therefore, the Morse force vector, being affected by the Morse force of diamond cutting tool, at the newly moved position of each atom in workpiece is one by one added to the Morse force of other workpiece atoms being inside cut-off radius borne by the newly moved position of each atom, so as to find the sum of Morse force vector of each workpiece atom, which is further decomposed to be Morse force component  $F_x$  in the X direction, Morse force component  $F_y$  in the Y direction, and Morse force component  $F_z$  in the Z direction. Let each of the Morse force components be zero, and then the force equilibrium equation of quasi-steady molecular statics nanocutting model can be acquired, as shown in equation (7).

$$F_X = \sum_{i=1}^m \vec{F}_{ix}(r_{ij}) = \sum_{i=1}^m \sum_{j=1}^n \delta F_x(r_{ij}) = 0 \quad (7)$$

$$F_Y = \sum_{i=1}^m \vec{F}_{iy}(r_{ij}) = \sum_{i=1}^m \sum_{j=1}^n \delta F_y(r_{ij}) = 0$$

$$F_Z = \sum_{i=1}^m \vec{F}_{iz}(r_{ij}) = \sum_{i=1}^m \sum_{j=1}^n \delta F_z(r_{ij}) = 0$$

where

$i$ : number assigned to all the atoms of diamond probe tool atoms that affect the Morse force of a certain workpiece atom

$j$ : number assigned to other workpiece atoms inside the cut-off radius after removal of a certain workpiece atom affected by Morse force of probe tool.

$m$ : quantity of all the atoms of diamond probe tool being corresponding to a certain workpiece atom affected by Morse force of probe tool.

$n$ : quantity of other workpiece atoms inside the cut-off radius after removal of a certain workpiece atom being influenced by Morse force of probe tool.

$r_{ij}$ : distance from the  $j^{th}$  workpiece atom in material and its corresponding  $i^{th}$  atom of diamond probe tool, and distance from the  $j^{th}$  workpiece atom and the  $i^{th}$  workpiece atom.

This paper uses Hooke-Jeeves pattern search method [Hooke and Jeeves (1961)] to look for the most suitable newly displaced position of each moved atom in workpiece of each step. Since the feeding of each step in the paper does not exceed 0.002Å, and the displacement of atom cannot be too far, the paper supposes that

the feeding of each search should not exceed the distance range of 1/2 lattice constant when searching the most suitable force balance transformation displacement position of each step. And Hook-Jeeves pattern search method is used to do the search. First of all, the starting point of search has to be defined. Let the workpiece atom affected by Morse force of diamond probe in each cutting step is taken as the starting point of the search. The increment of search is  $0.001\text{\AA}$ , and the convergence value of force equilibrium  $\varepsilon=10^{-6}$ . By following the above logic, the point of optimal displaced position for each step can be found. It is just the point of new force balance displaced position acceptable to us. During this time, the paper calculates the total Morse force borne by the interface between the workpiece and the cutting tool in the feeding step of this time. Furthermore, the total Morse force is decomposed to be component forces in X-, Y- and Z-directions, thus achieving the cutting force (component force in X-direction), cutting side force (component force in Y-direction) and cutting down force (component force in Z-direction).

### 3 Nanoscale cutting sapphire experiment by using AFM

In order to prove the simulation result of down force of three-dimensional quasi-steady molecular statics nanocutting of sapphire substrate, AFM probe is taken as the cutting tool to carry out nanocutting experiment. Besides, this paper also carries out experiment and verification of the SDFE theory and equation, proving that SDFE is approximately a constant value. The AFM equipment used in the experiment of this paper for machining is the commercial Dimension 3100 multimode AFM manufactured by Veeco Instruments Inc. The probe tool used is DT-NCHR diamond-coated probe produced by Nanosensors, with diamond coating at thickness 100 nm and a probe tip similar to a semisphere at radius of around 120 nm. Therefore, when machining workpiece by this probe, the probe tip is a cutting tool being similar to a semisphere.

The probe manufacturer provides the resonance frequency ( $f_v$ ) and spring constant ( $k_v$ ) of the probe for use in the experiment, being 320 kHz and 42 N/m respectively. In order to acquire the actual spring constant of probe ( $k_r$ ), this paper firstly uses a tapping mode AFM to make computer scanning, and then finds the actual resonance frequency ( $f_r$ ) of the probe used in the experiment. For the probe used in the experiment of the paper, the actual spring constant is  $k_r$ . Then, from the probe's resonance frequency ( $f_v$ ) and spring constant ( $k_v$ ) provided by the manufacturer, as well as the resonance frequency ( $f_r$ ) actually measured in the experiment, equation (8) is obtained:

$$\frac{f_v}{f_r} = \frac{\sqrt{k_r}}{\sqrt{k_v}} \quad (8)$$

where  $f_v$  is resonance frequency and  $k_v$  is normal spring constant which are provided by the manufacturer. For DT-NCHR diamond coated probe, the normal spring constant  $k_v$  provided by the manufacturer is 42 N/m, and the resonance frequency  $f_v$  provided by the manufacture is 320 kHz. The resonance frequency  $f_r$  is 310 kHz, which is measured by experiment. Thus, the normal spring constant can be calculated from equation (8), and the value of  $k_r$  is 39.3 N/m.

For the measurement way of down force applied on workpiece by AFM probe, the paper adopts the preset setpoint of AFM machine and uses the force curve displayed on AFM machine to measure the offset amount of probe cantilever under this setpoint. According to Dimension 3100 Manual of Veeco Digital Instruments Inc., through changing the setting of setpoint, we can adjust the feedback circuit kept by the deflection voltage of cantilever. Therefore, from the figure of force-calibration curve, the relationship between setpoint and the offset amount  $d$  of probe cantilever can be seen. When AFM is in force calibration mode, the parameter of setpoint is defined as a horizontal midline in the force calibration plot. Therefore, when setpoint is changed, the curve in the force calibration plot will move upwards and downwards. After the offset amount  $d$  of probe is measured and the spring constant  $k_r$  of probe is acquired from equation (8), the down force  $F_d$  ( $\mu\text{N}$ ) can be calculated from equation (9) (Sarid,1991).

$$F_d = k_r d \quad (9)$$

The machining way of nano V-shaped groove on sapphire substrate in the experiment of the paper is that after fixed down force is set, the required machining dynamic path of AFM probe and the steps required for machining are used to carry out program design. It is then linked to the built-in NanoLithography software of AFM machine, and machining can be immediately carried out. Besides, after this paper uses AFM probe to cut sapphire substrate, and uses AFM to conduct machining, the measurement experiment of the cutting depth and profile of sapphire substrate is performed.

#### **4 Theoretical model of SDFE and the calculating methods of down force and cutting depth of each pass**

##### ***4.1 The theoretical model of SDFE and the calculation method of removed volume***

This paper considers that in the actual nanoscale cutting process, machining in cutting directions is carried out by sufficient down force produced by the cutting tool of the probe onto the workpiece at a certain depth. On the workpiece being machined, the nanoscale particles of workpiece are moved and removed, which

is a mode of volume change. Therefore, in order to make it conform better to the physical phenomenon, this paper employed the concept of specific down force energy (SDFE) to approximately calculate the cutting depths of different cutting passes under fixed down forces. Conversely, if the cutting depth is fixed, SDFE theory can also be applied to approximately calculate the required down force for cutting workpiece.

This paper proposes the specific down force energy (SDFE) concept. SDFE is defined as being down force energy dividing the removed volume of down press of the workpiece by the AFM probe, and the down force energy can be obtained from the down force of the workpiece applied by the probe multiplying the down press depth. Thus, the equation of specific down force energy (SDFE) can be shown as equation (10):

$$\text{SDFE}(\text{specific down force energy}) = \frac{F_d \times \Delta d_n}{\Delta V_n} (\mu\text{N} \cdot \text{nm}/\text{nm}^3) \quad (10)$$

where  $F_d$  ( $\mu\text{N}$ ) is the down force applied by the AFM probe on the workpiece,  $\Delta d_n$  (nm) is the increased cutting depth in the  $n^{\text{th}}$  pass, and  $\Delta V_n$  ( $\text{nm}^3$ ) is the removed volume of down press of the workpiece in the  $n^{\text{th}}$  pass. Since the removed volume of down press of the workpiece changes with an increase in the cutting depth,  $\Delta V_n$  is the function of the cutting depth  $\Delta d_n$ .

This paper supposes that under the same workpiece material, the SDFE of the nanoscale cutting carried out under different down forces and repeated cutting operation procedures is close to a constant value. Besides, since the tip of the AFM probe is similar to a semispherical cutting tool, the removed volume of the workpiece by cutting in the first pass of machining can be acquired from the geometric equation of a sphere and the cutting of each pass is similar to the pressing of a semi-spherical cutting tool into the workpiece to carry out straight-line mobile machining. As observed from the sectional topography of groove depth in cutting direction after a cutting experiment, the cutting tool of the probe initially down presses into a shallower depth ( $d_i$ ). As the cutting tool moves, the cutting depth gradually increases from shallow to a constant value ( $d_1$ ) in the central region. Its removed volume also increases with greater cutting depth. This phenomenon is similar to the paper's model, which is simulated from the solid model actually constructed by CATIA CAD software. Therefore, the average depth measured and calculated by the paper by taking the central region's position of the machining groove as the cutting depth, conforms to the actual machining situation.

Therefore, the removed volume of down press in the first pass is initially a spherical cap with shallower down press depth (as shown in Fig. 3(a)). From the geometric relationship of contact between the cutting tool and the workpiece, it is known that

the initial removed volume of down press of the workpiece can be expressed as:

$$V_i = \pi d_i^2 \left( R - \frac{d_i}{3} \right) \quad (11)$$

where  $R$  is the tip radius of the cutting tool of the probe, and  $d_i$  is the initial indentation depth of the workpiece.

After the cutting tool moves, the down press depth in the central cutting region tends to be at a fixed cutting depth. Since the removed volume of indentation after the cutting tool has been removed from the earlier machining, the removed volume of down press during this time is the volume of the semispherical cap.

For the removal volume of the central region in the first pass, the forward distance of the radius of the spherical cap ( $r$ ) denotes the volume already removed. Thus, the removed volume during this time is 1/2 that of the spherical cap volume under a cutting depth (as shown in Fig. 3 (b)). The equation of its removed volume for the first pass is expressed as follows:

$$V_1 = \frac{1}{2} \pi d_1^2 \left( R - \frac{d_1}{3} \right) \quad (12)$$

where  $R$  is the tip radius of the cutting tool of the probe; and  $d_1$  is the cutting depth of the first pass.

Since the removed volume of down press..... above the second pass has gone through the removed groove of the previous pass, it is similar to a wedge in an arc. For this geometric shape, complicated integration has to be used to obtain the removed volume of down press. Therefore, this paper uses the geometric shape and down press depth of the cutting tool, and employs CAD software of CATIA to establish a solid model so as to carry out the simulation and calculation of the removed volume of down press. This paper proposes an important concept asserting that the removed volume of down press by the AFM probe for the specific down force energy in ( $i+1$ ) step is assumed that the position of the probe tip of AFM moves a radius distance of the spherical cap of the probe from the position of the probe tip of  $i$  step and then the removed volume of down press is calculated by CAD software. It is shown in Fig. 4.

#### **4.2 Calculation of down force using SDFE and calculation method of cutting depths for different cutting passes**

From equation (12), it is known that the removed volume of down press of the first cutting pass is the function of the cutting depth. Therefore, if the tip radius of AFM probe and the cutting depth  $d_1$  are both known, the removed volume of down

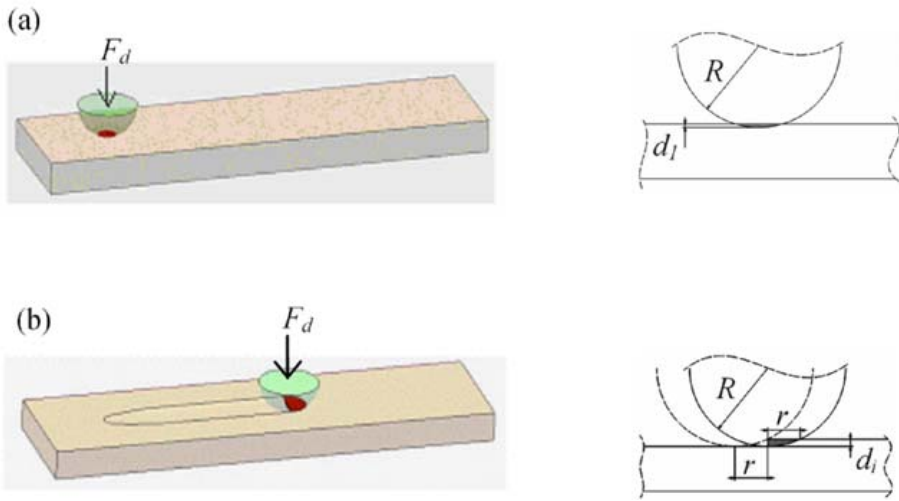


Figure 3: Schematic diagram and geometric relationship of the removed volume of down press of workpiece in (a) the first pass initially and (b) the central region of the first pass.

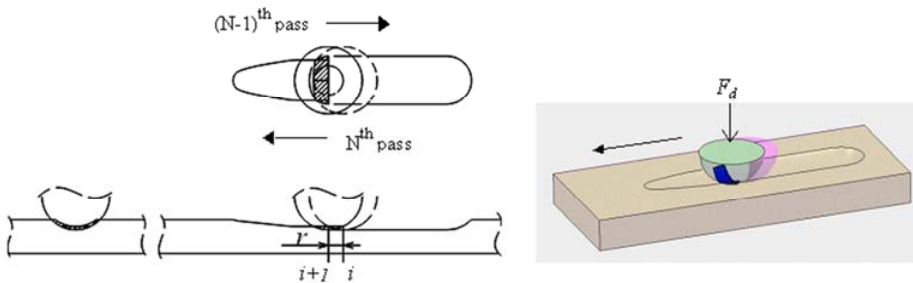


Figure 4: (a) The three views drawing and (b) schematic view of the removed volume of down press (black region) of the workpiece by the cutting tool of the AFM probe in a multi-passes machining.

press  $V_1$  can be calculated by equation (12). After that, the average SDFE ( $SDFE_r$ ) for nanocutting of sapphire substrate calculated by using the data acquired in the experiment of this paper as well as  $d_1$  and  $V_1$  already known above are substituted in equation (10), and then the down force ( $F_d$ ) required for cutting of sapphire in the first pass can be obtained.

Additionally, the removed volume above the second pass also changes with the

increase of the cutting depth. However, the integral equation of its removed volume is very complicated. Hence, the paper uses a step-by-step approximation method in an optimization calculation method, and takes the difference, acquired by deducting the calculated SDEF ( $SDFE_{cj}$ ,  $j=1,2,3\dots$ ) from the average SDFE obtained from the experiment ( $SDFE_t$ ), as the objective function, making it smaller or equal to the value ( $\varepsilon_{SDFE}$ ). It is also assumed that the convergence error is  $\varepsilon_{SDFE}=0.0003$  ( $\mu N \cdot nm/nm^3$ ) (as shown in equation 13). As for calculating the SDEF ( $SDFE_{cj}$ ,  $j=1,2,3\dots$ ), a known depth of the previous pass is increased step by step with an increment depth ( $\Delta d$ ). CAD software is used to calculate the removed volume of down press at each time of increment. After a step by step adjustment, this paper proposes increasing the increment of the down force depth to carry out a repeated calculation, making it approximate to the expected result of convergence error  $\varepsilon_{SDFE}$ , in order to forecast the cutting depth of each cutting pass.

$$|SDFE_t - SDFE_{cj}| \leq \varepsilon_{SDFE} \quad (13)$$

where  $SDFE_t$  is the average SDFE acquired from the experiment,  $SDFE_{cj}$  is the calculated SDFE of each increased depth; and  $\varepsilon_{SDFE}$  is the convergence error of the objective function.

From the cutting depth already known by calculation in the previous pass, an increment of depth ( $\Delta d_j$ ) is increased step-by-step. CAD software is used to calculate the removed volume of press at each increment of depth, as well as the calculated SDFE ( $SDFE_{cj}$ ,  $j=1,2,3\dots$ ) of this increment of the cutting depth and down press. This paper is step-by-step to adjust the increment of cutting depth and makes repeated calculation. When it approaches the expected convergent value of error ( $\varepsilon_{SDFE}$ ), the cutting depth of each cutting pass can be calculated approximately. Conversely, if the tip radius of AFM probe and the cutting depth of a certain cutting pass are both known, the removed volume of down press can be calculated using CAD software, and the required down force can be further calculated using equation (10) of SDFE.

## 5 Results and discussions

Below is an analysis made by this paper and based upon the cutting of different cutting depths on sapphire substrate workpiece by the cutting tool with different tip radii of probe according to the results of cutting force ( $F_x$ ), down force ( $F_y$ ) and side force ( $F_z$ ) acquired from simulation of three-dimensional quasi-steady molecular statics nanocutting model. Besides, this paper carries out AFM cutting experiment of multi-pass cutting on the surface of sapphire substrate by different down forces. According to the experimental results, it is proved that the average SDFE proposed

by this paper is approximately a constant value. Using the experimental data, the SDFE for cutting of sapphire substrate is calculated. Finally, the down force of nanocutting obtained by simulation calculation of the paper's three-dimensional quasi-steady molecular statics nanocutting model is compared with the down force calculated by the SDFE theoretical equation proposed by verification of the experimental result during actual nanocutting of sapphire substrate by AFM probe. It is found in the comparison that the down force acquired from the simulation result of this paper and the down force calculated by SDFE theory are very close. Therefore, it is proved that the three-dimensional quasi-steady molecular statics nanocutting theoretical model developed by this paper is feasible.

### ***5.1 Simulation results of 3D quasi-steady molecular statics nanocutting simulation model***

This paper establishes a three-dimensional quasi-steady molecular statics nanocutting simulation model for cutting of nano groove on the surface of sapphire by AFM probe. With tip radius of probe 5nm and cutting depth 0.5nm, as well as tip radius of probe 2nm and cutting depths 0.4nm, 0.5nm and 0.6nm, the paper conducts simulation analysis. Using the simulation results, the paper calculates the cutting force in X direction ( $F_x$ ), down force in Z direction ( $F_z$ ) and side force in Y direction ( $F_y$ ) under steady cutting condition. As to tip radii of probe 5nm and 2nm, as well as cutting depth 0.5nm, the simulation results of different steps are shown in Fig. 5.

According to the three-dimensional quasi-steady molecular statics nanocutting simulation model of sapphire developed by this paper, this paper simulates a tip radius of probe 5 nm to carry out sapphire cutting process at a cutting depth 0.5 nm, and simulates a tip radius of probe 2 nm to carry out sapphire cutting process at cutting depths 0.4 nm, 0.5 nm and 0.6 nm. The acquired results of cutting force ( $F_x$ ), down force ( $F_z$ ) and side force ( $F_y$ ) of each step in three axial directions are respectively obtained, as shown in Figures 6~9. From the simulation results, it is found that under the conditions that both the tip radii of probe and cutting depths are different, despite the constant change of force in the Y-direction, the average value is close to zero. This is because the tool used in the simulation of cutting performed has a rounded tip, and the cutting path is a straight line. Therefore, the contact areas at its two sides during cutting are the same, and the resultant action force at each of the ends is zero.

From Fig. 6 to Fig. 9, it can be found that the action forces in X-and Z-directions are negative values at the beginning stage of nanoscale cutting. This is because in the initial stage of cutting, the probe tool is maintained at a small distance from the workpiece, so a mutual attraction is produced between the cutting tool and the workpiece, generating negative values. However, after the tool cuts the workpiece,

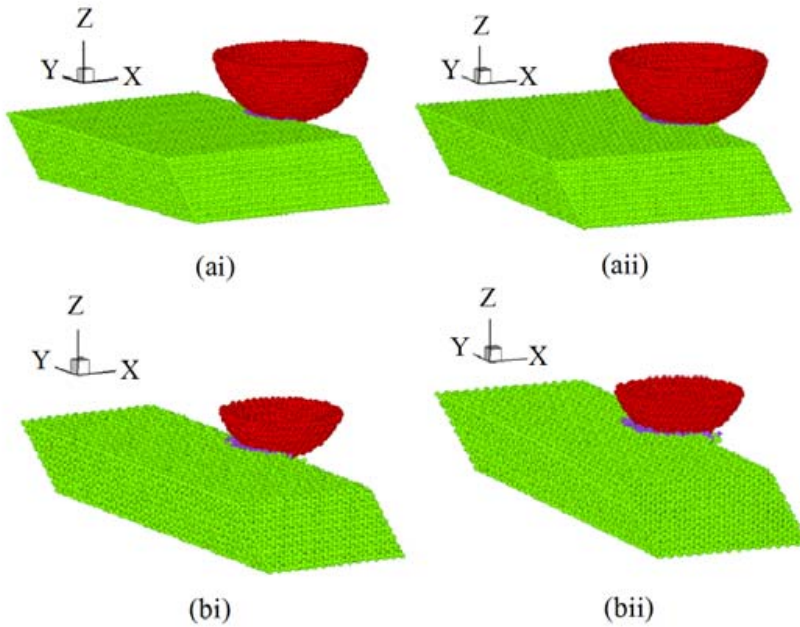


Figure 5: Simulated results of different tip radius and different steps at depth of cut 0.5nm. (ai) The tip radius is 5nm and the 6000<sup>th</sup> step. (aai) The tip radius is 5nm and the 12000<sup>th</sup> step. (bi) The tip radius is 2nm and the 5000<sup>th</sup> step. (bii) The tip radius is 2nm and the 9500<sup>th</sup> step.

such that the values of force are positive. At the same time, it is also found that the absolute values of down forces of different cutting depths in the Z-direction are greater than the absolute values of cutting forces in the X-direction, because, when the conical tool begins cutting the workpiece, the projected contact area in the Z-direction is greater than the projected contact area in the X-direction. Therefore, in the initial cutting stage, the attraction force (negative value) in Z-direction is greater than the attraction force (negative value) in X-direction. As the probe tool gradually cuts the workpiece, a repulsive force is produced between the cutting tool and the workpiece. Since the projected contact area in the Z-direction is greater than the projected contact area in the X-direction, the repulsive force is also greater. Therefore, it is found that the increase rate of the down force in the Z-direction is greater than that of the cutting force in the X-direction.

From Fig. 6 to Fig. 9, the simulation conditions of different tip radii of probe and different cutting depths are shown. The contacted crown radii of cutting tools

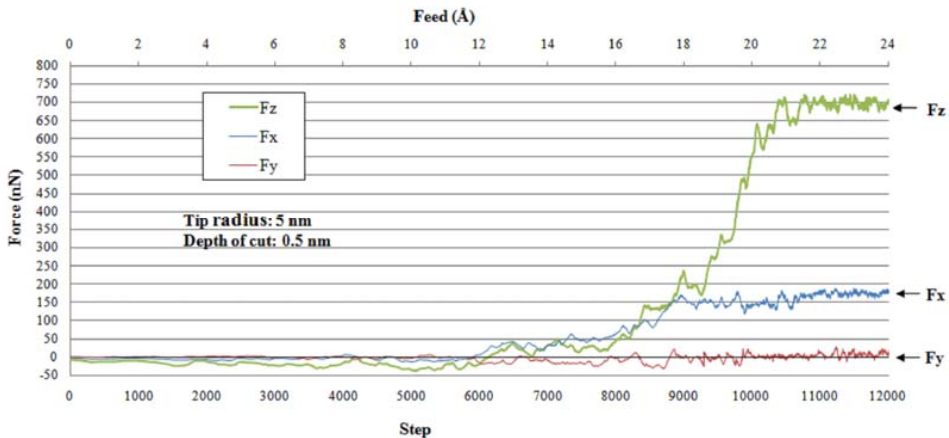


Figure 6: Three axial action forces when tip radius of probe is 5 nm and cutting depth is 0.5nm.

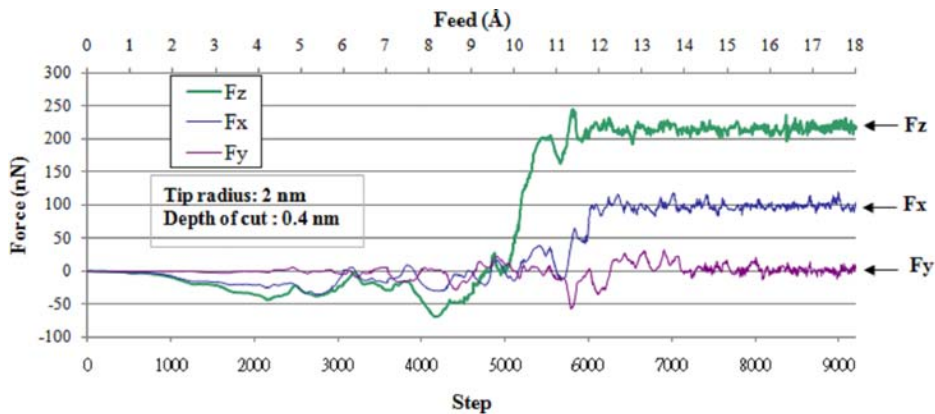


Figure 7: Three axial action forces when tip radius of probe is 2 nm and cutting depth is 0.4nm.

during simulation of cutting sapphire workpiece by the tip of probe are 1.96nm, 1.2nm, 1.32nm and 1.43nm respectively. When simulation at the 10900<sup>th</sup>, 6200<sup>th</sup>, 6800<sup>th</sup> and 7300<sup>th</sup> step, the length on workpiece cut by probe tool exceeds the crown radii respectively. During this time, the force also starts to be in steady condition. The down force  $F_z$  and the average action force of cutting force  $F_x$ , obtained under the cutting condition that different tip radii of probe and different cutting depths appear to be steady, are further rearranged and shown in Table 3.

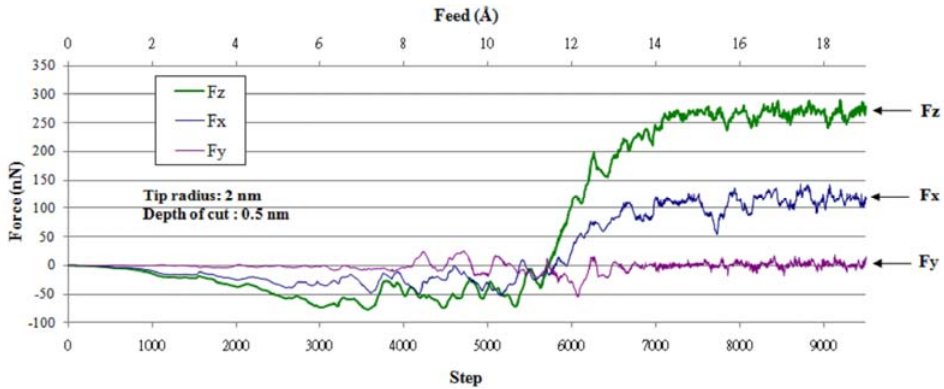


Figure 8: Three axial action forces when tip radius of probe is 2 nm and cutting depth is 0.5nm.

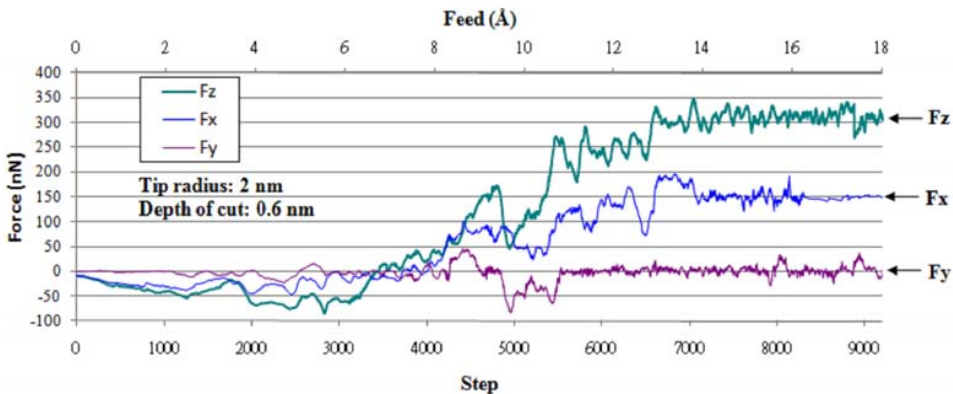


Figure 9: Three axial action forces when tip radius of probe is 2 nm and cutting depth is 0.6nm

## 5.2 Experimental result and analysis of specific down force energy theoretic model

Focusing on the sapphire substrate, and using the various down forces of AFM probe acquired by using different setpoints, being 32.67, 42.37, 49.10 and 51.10  $\mu\text{N}$  respectively, the paper conducts experiment of to-and-fro cutting for 1~5 passes. The individual profile and depth of the middle cross-section of the V-shaped groove after cutting are shown in Fig. 10. The various cutting depths of different cutting passes measured in related experiments and the calculation results after compared with the related theoretical equations are shown in Tables 4 to 7.

Table 3: Average down force and average cutting force under different cutting conditions as simulated by this paper.

Computational parameters		Down force : Fz (nN)	Cut force : Fx (nN)
Tip radius (nm)	Depth of cut (nm)		
5	0.5	696.24	150.2
2	0.4	215.43	97.72
2	0.5	261.18	109.06
2	0.6	312.11	148.76

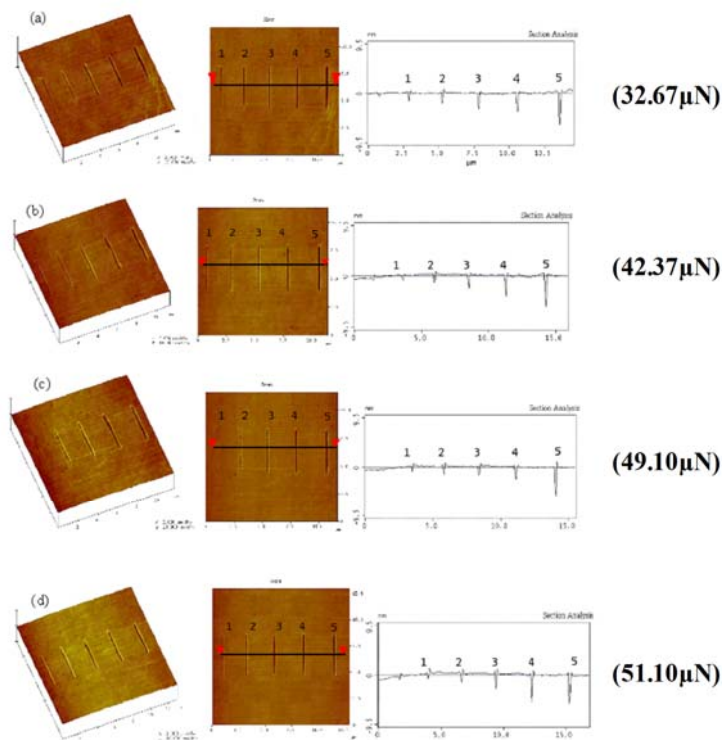


Figure 10: Images of machining depths of the 1<sup>st</sup> ~ 5<sup>th</sup> steps measured by AFM under different down forces.

From Table 4, we can see the cutting depth of nano groove measured after the first cutting pass under four different down forces. The removed volume of press of workpiece calculated by the actual model constructed by CAD software is compared with the removed volume of press calculated by theoretical equation (12),

Table 4: Measured and calculated data of the first pass under different down forces in experiments

Down force ( $\mu\text{N}$ )	Experimental and measured depth of the first pass (nm)	Removed volume of material calculated by CAD ( $\text{nm}^3$ )	Removed volume of material calculated by equation (12) ( $\text{nm}^3$ )	SDFE simulated and material calculated by CAD ( $\mu\text{N} \cdot \text{nm} / \text{nm}^3$ )	SDEF calculated by the theoretical equation (10)
32.67	0.951	170.01	170.02	0.1827	0.1827
42.37	1.235	286.35	286.51	0.1827	0.1826
49.10	1.429	383.49	383.42	0.1829	0.1829
51.10	1.489	416.28	416.30	0.1827	0.1827

and the two data are found to be very close, revealing that it is reasonable for this paper to construct and calculate the removed volume of press by CAD. Table 4 also shows that after the calculated removed volume is substituted in the SDFE equation (10) proposed by this paper, the numerical SDFE values of the nanocutting of sapphire substrate after the first cutting pass under different down forces are very close to each other, just meeting the supposition made by the paper. Therefore, for the constant value of SDFE, this paper takes its average value to be approximately  $0.1827(\mu N \cdot nm/nm^3)$ .

Table 5: Relationship between cutting depth under down force  $42.37\mu N$  in multi-pass cutting experiment and the calculated removed volume and SDFE.

Down force	Number of cutting passes	Experimental measured depth (nm)	Removed volume calculated by CAD ( $nm^3$ )	SDFE ( $\mu N \cdot nm/nm^3$ )
	1	1.235	286.35	0.1827
	2	1.621	89.23	0.1828
$42.37\mu N$	3	1.925	70.67	0.1829
	4	2.185	60.32	0.1826
	5	2.425	55.64	0.1827

Table 6: Relationship between cutting depth under down force  $49.10\mu N$  in multi-pass cutting experiment and the calculated removed volume and SDFE.

Down force	Number of cutting passes	Experimental measured depth (nm)	Removed volume calculated by CAD ( $nm^3$ )	SDFE ( $\mu N \cdot nm/nm^3$ )
	1	1.429	383.49	0.1829
	2	1.879	120.98	0.1826
$49.10\mu N$	3	2.229	93.86	0.1829
	4	2.539	83.17	0.1827
	5	2.809	72.38	0.1826

Table 5 and Table 6 show the data of cutting depths of the first to fifth cutting passes measured under the fixed down forces  $42.37\mu N$  and  $49.1\mu N$  respectively, as well as the removed volume of press under multi-pass cutting calculated by the solid model established by CATIA's CAD software. Tab. 5 and Tab. 6 also show the numerical SDFE value of each cutting pass calculated by SDFE equation (10). The results show that the SDFE of each different cutting pass is also quite close to a

constant value. The average SDFE of each pass under these two down forces is also  $0.1827(\mu\text{N} \cdot \text{nm}/\text{nm}^3)$ .

Focusing on down forces  $42.37\mu\text{N}$  and  $49.1\mu\text{N}$ , this paper uses stepwise approximation method to step by step increase the cutting depth of the fourth pass. Furthermore, CAD software is used to calculate the volume of the cutting depth increment, thus acquiring the cutting depth of the fifth pass and the SDFE of the removed volume, which is then compared with the average SDFE obtained from experiment and the calculated SDFE of the 5<sup>th</sup> step. From the error function equation (13) of SDFE, the range of cutting depth increment is revised time after time in order to approach to the error convergence  $\varepsilon_{SDFE}$  of SDFE. Finally, the cutting depths of the fifth pass calculated by the theoretical model under down forces  $42.37\mu\text{N}$  and  $49.1\mu\text{N}$  are 2.455 and 2.793 nm respectively, which form an error of 0.3~1.2% when compared with the cutting depths 2.425nm and 2.809nm measured in the experiment. Since the error is very small, it is proved that it is feasible for the paper to step by step approach to the error function equation (13) by increasing the cutting depth increment, and use CAD software to calculate the removed volume of press under multi-pass cutting and calculate the SDFE model.

In order to further prove the proposed SDFE theory, the paper takes the acquired average SDFE  $0.1827(\mu\text{N} \cdot \text{nm}/\text{nm}^3)$  of nanocutting of sapphire substrate to calculate the cutting depth 1.49 nm of the first pass under down force  $51.1\mu\text{N}$ . The cutting depth acquired in the first pass is step by step increased. CAD software is employed to calculate the removed volume after depth increase and the SDFE under this depth. Depth is step by step increased to approach to the error function of SDFE of equation (13). In this way, the cutting depths of the second to the fifth pass are calculated, as shown in Table 7. Table 7 shows the cutting depth of each pass calculated by theoretical equation and the cutting depth measured in experiment. Between them, the average error is 0.62%. Since the error in between is very small, it is proved that the SDFE theory proposed by this paper is quite reasonable, and the cutting depths of different cutting steps under different down forces can be predicted.

Under the conditions that the geometric shape of probe tool and cutting depth are both known, this paper can calculate the down force of cutting depth of the first pass using the proposed SDFE theoretical equation (10) as well as equation (12) of the removed volume of press of the first cutting pass. From the results in Table 8, it is seen that the cutting depth of the first cutting pass is measured in the experiment of this paper. The cutting down force calculated by the aforementioned calculation method of cutting down force is compared with the actual down force of AFM probe set for the experiment of the paper, and the average error in between is around 0.37%. Therefore, since the calculated result of down force is very close to the

Table 7: Difference between experimental measurement and SDFE theoretical calculation of cutting depths for each pass under down force of  $51.1\mu\text{N}$ .

Down force	The number of cutting passes	Cutting depth measured by AFM (nm)	Cutting depth calculated by SDFE theoretical model (nm)	Difference of cutting depth between that measure by AFM and calculated by SDFE model (%)
$51.1\mu\text{N}$	1	1.489	1.49	0.06
	2	1.963	1.95	0.70
	3	2.335	2.32	0.67
	4	2.671	2.65	0.81
	5	2.940	2.915	0.85

down force actually set, it reveals that the SDFE theoretical model proposed by this paper can predict the cutting down force under the conditions that the geometric shape of cutting tool and cutting depth are both known.

Fig. 11, Fig. 12 and Fig. 13 show the analytic results of nanocutting experiment of sapphire substrate carried out by this paper. From Fig. 11, it can be seen that cutting depth deepens with the increase of cutting passes. From Fig. 12, it can be seen that cutting depth deepens with the increase of cutting down force. From Fig. 13, it can be seen that the increased depth ( $\Delta d_i$ ) of each pass tends to decrease with the increase of cutting passes.

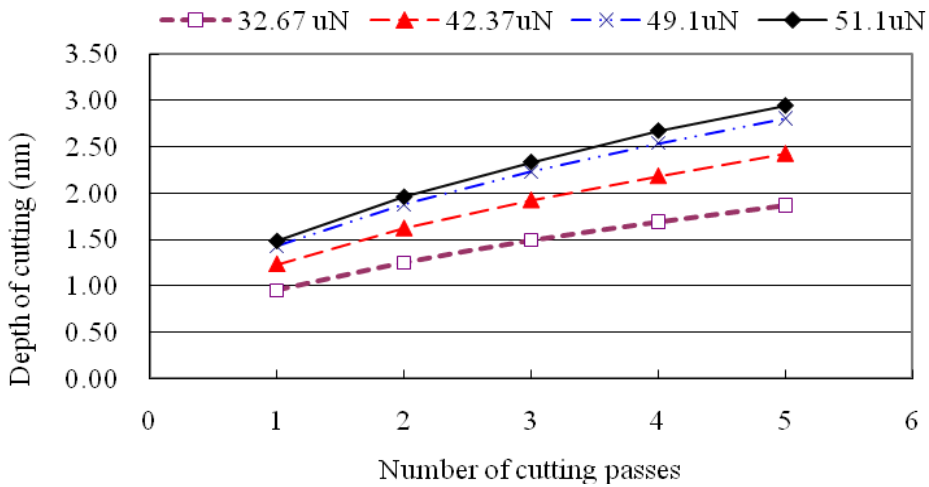


Figure 11: Relationship between the cutting depth and the number of cutting passes.

### 5.3 Simulation results and verification of calculation result after application of SDFE theory

The paper verifies the feasibility of the three-dimensional quasi-steady molecular statics nanocutting simulation model of sapphire developed within it. Therefore, the average down force acquired from simulation calculation is compared with the down force calculated by SDFE theoretical model which is innovatively proposed from the experimental result of actual cutting of sapphire substrate. Under the conditions that the tip radii of probe are 5 nm and 2 nm, and the cutting depths are 0.4 nm, 0.5 nm and 0.6 nm. Table 9 shows the down force calculated based on the down force acquired from simulation calculation by three-dimensional quasi-steady

Table 8: Error between down force of the first cutting pass calculated by SDFE theoretical equation and actual down force in the experiment.

The radius of tip (mm)	The removal volume calculated by equation (12) (mm <sup>3</sup> )	Experimental and measured depth of the first pass (mm)	The down force set by experiment ( $\mu$ N)	The down force calculated by theoretical equation (10) ( $\mu$ N)	Difference between the down forces calculated and experimental set (%)
120	169.48	0.951	32.67	32.56	0.336
120	285.60	1.235	42.37	42.25	0.283
120	382.17	1.429	49.1	48.86	0.487
120	414.86	1.489	51.1	50.90	0.384

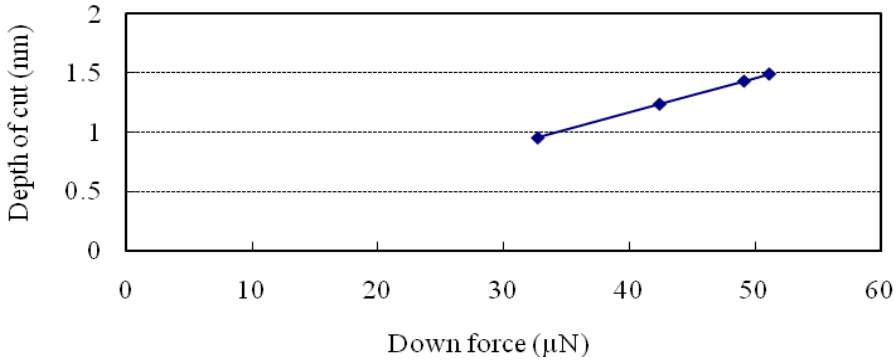


Figure 12: Relationship between the cutting depth and the down force.

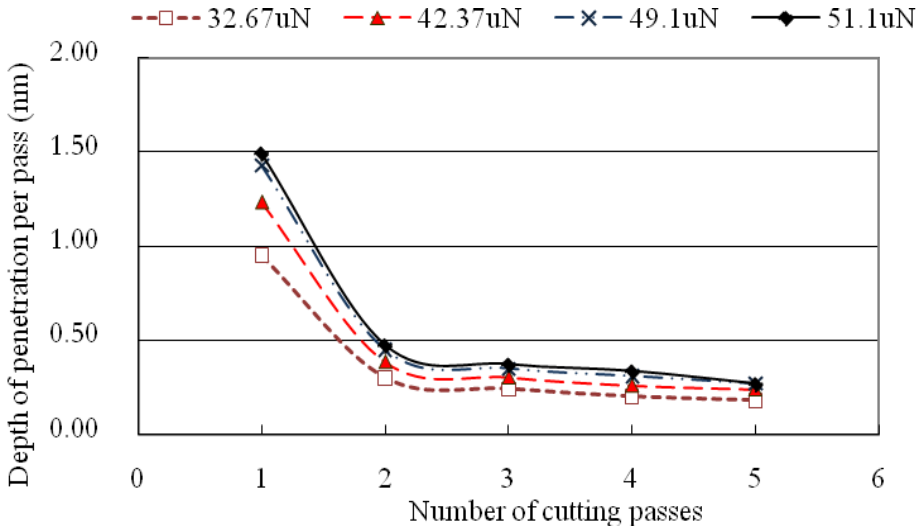


Figure 13: Relationship between increased cutting depth and number of cutting passes.

molecular statics nanocutting of sapphire workpiece and the down forces calculated based on the value of SDFE  $0.1827 (\mu\text{N} \cdot \text{nm}/\text{nm}^3)$  acquired from the cutting of sapphire substrate and SDFE equation (10). As seen from Table 9, the average error between the down force calculated by SDFE method and the down force calculated by three-dimensional quasi-steady molecular statics model is around 1.85%. The very small error between them reveals that it is reasonable and acceptable for this paper to use three-dimensional quasi-steady molecular statics model to simulate a

nanocutting simulation for cutting sapphire substrate.

## 6 Conclusion

This paper proposes using the three-dimensional quasi-steady molecular statics nanocutting model to simulate application of AFM diamond probe to conduct straight-line nanocutting of sapphire substrate. From the simulation results of cutting force, down force and side force, it is found that under the same tip radius of probe, cutting force enlarges with the increase of cutting depth. This result is identical to the actual experimental phenomena of nanocutting of sapphire. For the average action forces in different axial directions after cutting is steady, the average side force in the Y-direction is around zero, and the down force in the Z-direction is greater than the cutting force in the X-direction. This is because in the cutting process of the conical tool, the projected contact area between cutting tool in the Z-direction and the workpiece is greater than the projected contact area between cutting tool in the X-direction and the workpiece.

Meanwhile, this paper takes AFM diamond-coated probe as the cutting tool to carry out nanocutting experiment of sapphire substrate, and further innovatively proposes the SDFE theory of nanocutting. From the data of experimental results, it is found that with the same probe tool used and under different cutting down forces and different cutting passes, the average SDFE obtained from calculation during nanocutting of sapphire is close to the constant value  $0.1827(\mu N \cdot nm/nm^3)$ . This SDFE theoretical method can be applied to predict the required down force for reaching a certain cutting depth under the condition that the geometric shape of probe is known. Besides, from the down force set, the cutting depth of each different cutting step can be estimated. The paper uses the down force calculated by such SDFE theoretical model to prove the down force acquired by simulation calculation of this paper's three-dimensional quasi-steady molecular statics nanocutting model. It is also found that the error between the down force calculated by SDFE theoretical equation and the down force simulated by three-dimensional quasi-steady molecular statics nanocutting model is very small. It is known that AFM cannot measure cutting force in the X-direction and side force in the Y-direction. However, three-dimensional quasi-steady molecular statics nanocutting model is established by firstly making simulation calculation of total component forces during cutting, and then decomposing it to be cutting force in the X-direction, down force in the Z-direction and side force in the Y-direction. Therefore, as acquired from simulation, the down force in the Z-direction and the down force acquired from calculation of SDFE theoretical equation are quite close. Then, it can be reasonably interpreted that the cutting force in the X-direction acquired from simulation calculation and the side force in the Y-direction are both reasonably acceptable values. Thus, the

Table 9: Down force acquired from simulation calculation of three-dimensional quasi-steady molecular statics model and down force calculated by SDFE equation, as well as the error between them.

Tip radius (nm)	Cutting depth (nm)	Down force calculated by simulation (nN)	Down force calculated by SDFE equation (nN)	Difference between the down forces calculated by simulation and SDFE equation %
5	0.5	705.32	693.54	1.70
2	0.4	217.86	214.28	1.67
2	0.5	268.24	263.07	1.97
2	0.6	316.43	309.94	2.09

three-dimensional quasi-steady molecular statics nanocutting simulation model for nanocutting the sapphire substrate used by this paper is reasonable. The proposed SDFE theoretical model can be applied to predict the down force for nanocutting the sapphire substrate with the shape and dimensions of probe being known and the cutting depth being known. Besides, the theoretical model of SDFE can also be used to predict the cutting depths of different cutting passes with the down force being set.

**Acknowledgement:** The authors would like to give special thanks to the National Science Council, Taiwan, R.O.C., for financial support through Contract No. NSC 99-2221-E-011-019.

## References

**Belak, J. ; Stowers, I. F.** (1990): A Molecular Dynamics Model of the Orthogonal Cutting Process. *Proc. Am. Soc., Precision Eng.*, vol.389,pp.76-79.

**Childs, T. H. C. ; Maekawa, K.** (1990): Computer-aided Simulation and Experimental Studies of Chip Flow and Tool Wear in the Turning of Flow Ally Steels by Cemented Carbide Tools. *Wear*, vol. 139, no.2, pp. 235-250.

**Cai, M. B.; Li, X. P.; Rahman, M.** (2007): Study of the mechanism of nanoscale ductile mode cutting of silicon using molecular dynamics simulation. *International Journal of Machine Tool & Manufacture*, vol.47, pp.75-80.

Digital Instruments, Dimension™ 3100 Manual. Version 4.43B, Digital Instruments Veeco Metrolgy Group, 2000.

**Fang, F.Z.; Wu, H.; Zhou, W. X. T. Hu, X.T.** (2007): Modeling and experimental investigation on nanometric cutting of monocrystalline silicon. *Journal of Materials Processing Technology*, vol.184, no.1-3, pp. 407-410.

**Fang, T. H.; Weng, C. I.; Chang, J. G.** (2000): Machining characterization of nano-lithography process by using atomic force microscopy. *Nanotechnology* , vol. 11, pp.181-187.

**Girifalco, L. A.; Weizer, V. G.** (1959) : Application of the Morse Potential Function to Cubic Metals. *Phys. Rev.*, vol.114, no.3, pp.687-690.

**Graves, D.B.; Brault, P.** (2008): Molecular dynamics for low temperature plasma-surface interaction studies. *Journal of Physics D: Applied Physics*, vol. 42, pp. 194011.

**Hooke, R.; Jeeves, T. A.** (1961): Direct search solution of numerical and statistical problem. *Journal of the Association for Computing Machinery*, vol. 8, pp.212-229.

**Irving, J. H.; Kirkwood, J. G.** (1950): The statistical mechanical theory of trans-

port properties. IV. The equations of hydrodynamics. *J. Chem. Phys.*, vol. 18, pp. 817-829.

**Inamura, T.; Takezawa, N.** (1991): Cutting Experiments in a Computer Using Atomic Models of a Copper Crystal and a Diamond Tool. *Int. J. Japan Soc. Prec. Eng.*, vol. 25, no. 4, pp. 259-266.

**Inamura, T.; Takezawa, N.** (1992): Atomic-Scale Cutting in a Computer Using Crystal Models of Copper and Diamond. *Annals of the CIRP*, vol. 41, no. 1, pp. 121-124.

**Inamura, T.; Takezawa N.; Kumaki, Y.** (1993): Mechanics and energy dissipation in nano scale cutting. *Annals. CIRP*, vol.42, no.1, pp.79-82.

**Imafuku, M.; Sasajima, Y.; Yamamoto, R.; Doyama, M.** (1986): Computer simulations of the structures of the metallic superlattices Au/Ni and Cu/Ni and their elastic moduli. *J. Phys. F: Met. Phys.*, vol. 16, 823.

**Jeng, Y. R.; Tan, C. M.** (2004): Study of Nanoindentation Using FEM Atomic Model. *Journal of Tribology*, vol. 126, pp. 767-774.

**Kwon, Y. W.; Jung, S. H.** (2004): Atomic model and coupling with continuum model for static equilibrium problem. *Computers and Structures*, vol.82, pp. 1993-2000.

**Lin, Z. C.; Huang, J. C.** (2004): A nano-orthogonal Cutting Model Based on a Modified Molecular Dynamics Technique. *Nanotechnology*, vol. 15, pp. 510-519.

**Lin, Z. C.; Ye, J. R.** (2009): Quasi-steady molecular statics model for simulation of nanoscale cutting with different diamond cutter. *CMES: Computer Modeling in Engineering & Sciences*, vol.50, no.3, pp.227-252.

**Lin, Z. C.; Wang, R. Y.** (2010): Three Dimensional Nanoscale Abrasive Cutting Simulation and Analysis for Single-Crystal Silicon Workpiece. *CMC: Computers, Materials & Continua*, vol.16, no.3, pp.247-272

**Maekawa, K.; Itoh, A.** (1995): A friction and tool wear in nano-scale machining - A molecular dynamics approach. *Wear*, vol. 188, pp. 115-122.

**Shimada, S.** (1990): Molecular Dynamics Analysis as Compared with Experimental Results of Micromachining. *Ann. CIRP*, vol.41, no. 1, pp.117-120.

**Shackelford, James F.** (1988): *Introduction to Materials Science for Engineers (2nd ed.)*, Macmillan Inc., N.Y., PP. 93-94.

**Sarid, D.**: *Scanning Force Microscopy*. Oxford University Press, New York, (1991).

**Tseng, A. A.; Jou, S.; Notargiacomo, A., Chen, T.P.** (2008): Recent developments in tip-based nanofabrication and its roadmap. *J. Nanosci. Nanotechnol.* vol. 8, pp.2167-2186.

**Tseng, A. A.** (2010): A comparison study of scratch and wear properties using atomic force microscopy. *J. Applied Surface Science*, vol. 256, pp. 4246- 4252.

**Wang, Z. Q.; Jiao, N. D.; Tung, S. Dong, Z. L. (2010): Research on the atomic force microscopy-based fabrication of nanochannels on silicon oxide surfaces. *Chinese Science Bulletin*, vol. 55, pp. 3466-3471.**